GEOLOGICAL SURVEY OF FINLAND
Report of Investigation 181
2010

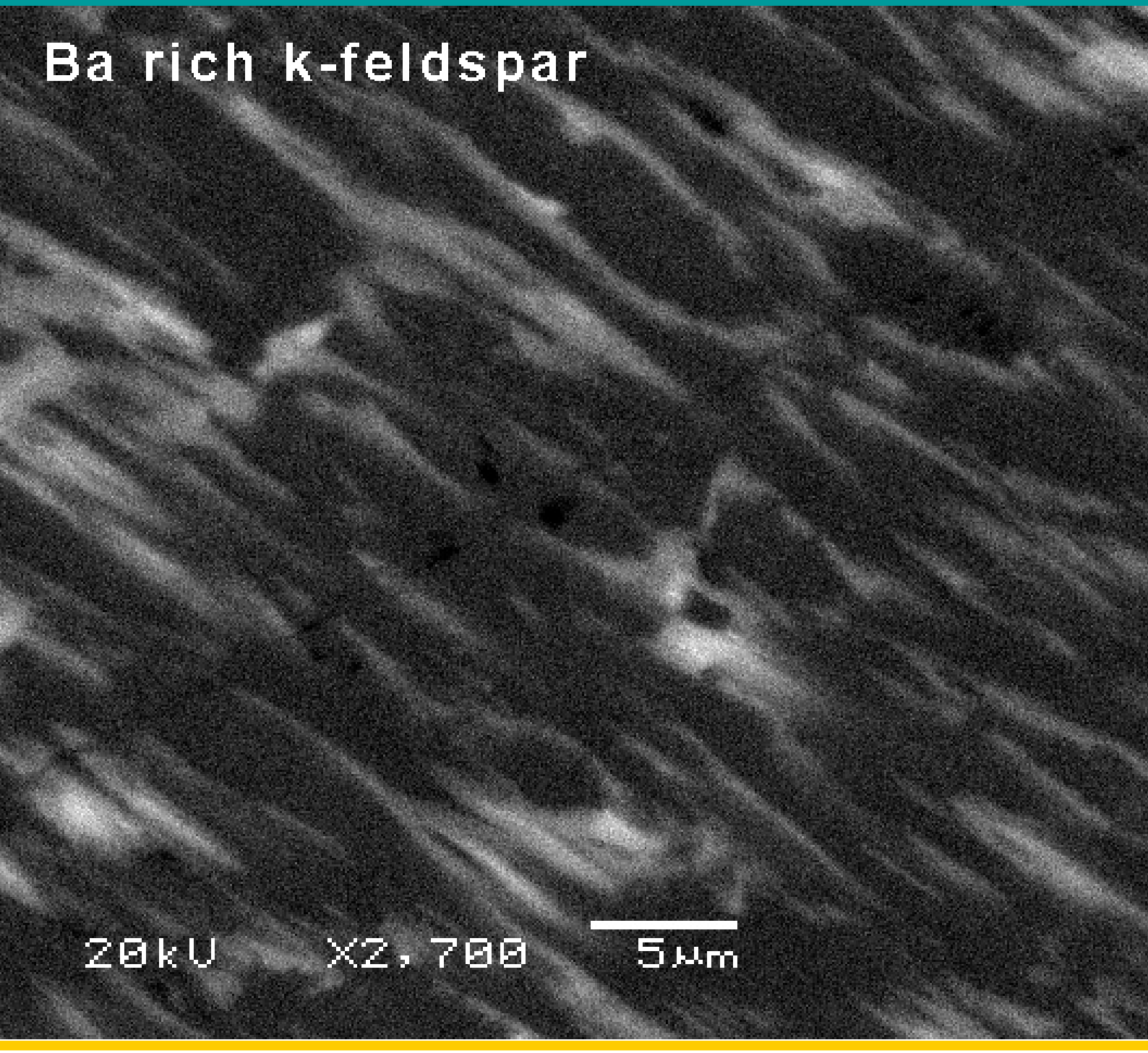

Barium-bearing alkali feldspar in the Lumikangas gabbro, Kauhajoki, Western Finland

Tegist Chernet

GTK

GEOLOGIAN TUTKIMUSKESKUS

Tutkimusraportti 181

GEOLOGICAL SURVEY OF FINLAND

Report of Investigation 181

Tegist Chernet

BARIUM-BEARING ALKALI FELDSPAR IN THE LUMIKANGAS GABBRO, KAUHAJOKI, WESTERN FINLAND

Espoo 2010

Chernet, T. 2010. Barium-bearing alkali feldspar in the Lumikangas gabbro, Kauhajoki, Western Finland. *Geological Survey of Finland, Report of Investigation 181,* 16 pages, 10 figures and 5 tables.

An elevated content of potassium (K) and barium (Ba) in whole rock analyses and a high content of BaO associated with alkali feldspar initiated a mineralogical investigation of the Lumikangas ilmenite-magnetite-apatite mineralized gabbro. Potassium feldspar/barian orthoclase ($Cn_{1–12}An_{0–3}Ab_{3–28}Or_{63–96}$), hyalophane ($Cn_{15–21}An_{0–3}Ab_{10–19}Or_{62–71}$), albite ($An_{6–9}Ab_{91–94}Or_{0–1}$) and oligoclase ($Cn_{0–1}An_{13–29}Ab_{71–86}Or_{0–3}$) compositions appear to coexist in the barium-bearing alkali feldspar (potassium feldspar = Orthoclase (Or), albite (Ab), anorthite (An) and celsian (Cn)). Barium- bearing potassium feldspar occurs in unexsolved, perthite, antiperthite and mesoperthite structures.

The presence of magmatic alkali feldspar, as well as its composition and textural properties in the Lumikangas gabbro, suggest crystal accumulation during the last stages of crystallization from a magma. The barium-rich potassium feldspar variety indicates a comparatively high concentration of barium in the late-stage liquids. Associated interstitial quartz, slight albitization of plagioclase and secondary zoning of plagioclase in contact with alkali feldspar are evidence that crystal cumulates reacted with late-stage melts or possibly with late infiltrated hydrothermal fluids.

Keywords (GeoRef Thesaurus, AGI): gabbros, alkali feldspar, K-feldspar, barium feldspar, hyalophane, electron probe data, magmatism, crystallization, Lumikangas, Kauhajoki, Finland

Tegist Chernet
Geological Survey of Finland
P.O. Box 96
FI–02151 Espoo
Finland

E-mail: tegist.chernet@gtk.fi

ISBN 978-952-217-117-7 (PDF)
ISSN 0781-4240

Chernet, T. 2010. Barium-bearing alkali feldspar in the Lumikangas gabbro, Kauhajoki, Western Finland. *Geologian tutkimuskeskus, Tutkimusraportti 181,* 16 sivua, 10 kuvaa ja 5 taulukkoa.

Lumikankaan ilmeniitti-magnetiitti-apatiittigabron kohonneet K- ja Ba-pitoisuudet sekä kalimaasälvän korkea Ba-pitoisuus käynnistivät tämän mineralogisen tutkimuksen. Kalimaasälpä / bariumortoklaasi ($Cn_{1–12}An_{0–3}Ab_{3–28}Or_{63–96}$), hyalofaani ($Cn_{15–21}An_{0–3}Ab_{10–19}Or_{62–71}$), albiitti ($An_{6–9}Ab_{91–94}Or_{0–1}$) ja oligoklaasi ($Cn_{0–1}An_{13–29}Ab_{71–86}Or_{0–3}$) näyttävät esiintyvän yhdessä bariumpitoisen kalimaasälvän kanssa (kaliummaasälpä = ortoklaasi (Or), albiitti (Ab), anortiitti (An) ja selsiaan (Cn). Bariumpitoinen kalimaasälpä esiintyy suotautumattomissa pertiitti-, antipertiitti- sekä mesopertiittirakenteissa.

Magmaattisen kalimaasälvän esiintyminen sekä Lumikankaan gabron koostumus ja tekstuuri viittaavat muodostumiseen magman kiteytymisen lopussa. Tämän kalimaasälpätyypin esiintyminen on osoitus bariumin konsentroitumisesta sulaan kiteytymisen lopulla. Kalimaasälvän yhteydessä esiintyvä interstitiaalinen kvartsi, hiukan albiittiutunut plagioklaasi ja sen sekundaarinen vyöhykkeisyys osoittavat kumulusfaasien reagoineen myöhäisen vaiheen sulan tai hydrotermisten fluidien kanssa..

Asiasanat (Geosanasto, GTK): gabrot, alkalimaasälvät, kalimaasälpä, bariummaasälvät, hyalofaani, elektronimikroanalysaattoritiedot, magmatismi, kiteytyminen, Lumikangas, Kauhajoki, Suomi

Tegist Chernet
Geologian tutkimuskeskus
PL 96
02151 Espoo
Suomi

Sähköposti: tegist.chernet@gtk.fi

CONTENTS

1 INTRODUCTION

X-ray fluorescence analyses along drill core samples from the Lumikangas gabbro in western Finland indicates Ba-enrichment, where the Ba-concentration increases with an increasing K-content. The Ba-content of the Lumikangas gabbro varies from one drill core to another, and even along the same drill core. According to XRF analyses, the Ba-content along four drill cores ranges from 0.02 to 0.145 %. Selected representative analyses are presented in Table 1. Petrographic analyses further reveal the presence of alkali feldspar with a considerable amount of barium (up to 5.7 wt% BaO) in the upper part of the intrusion (Sarapää et al. 2005). Barian silicates are rare and most commonly occur in association with manganese deposits (Deer et al. 1967). Barium feldspars, however, are described to occur in diverse settings, such as in metasediments, carbonates, hydrothermal veins, granites, pegmatites and felsic volcanic rocks (Frondel et al. 1966, Bjoerlykke & Griffin 1973, Němec 1975, Shmakin 1979, Essene et al. 2005). The coexistence of potassium feldspar and hyalophane is of considerable petrographic interest and of great importance in unravelling clues to the crystallization and thermal history of igneous and metamorphic rocks.

Table 1. Selected results of XRF chemical analyses of Lumikangas ilmenite-magnetite-apatite ore from four drill cores.

	1	2	3	4	5	6	7	8	9	10	11
Na_2O	2,19	2	1,9	1,02	2,34	2,49	2,44	3,14	2,23	2,43	2,88
MgO	6,4	7,14	6,9	8,01	4,85	4,53	4,98	4,12	6,56	5,58	4,26
Al_2O_3	12,6	11,5	11,1	6,90	11,6	12,2	12,0	16,1	11,7	13,7	14,9
SiO_2	40,1	35,4	36,3	34,6	40,4	42,9	41,7	44,7	41,2	40,8	41,0
P_2O_5	2,201	3,596	3,372	0,782	2,87	2,59	2,67	1,39	1,80	1,94	1,52
K_2O	0,865	0,473	0,572	0,195	0,977	1,48	1,23	1,05	0,978	0,895	0,61
CaO	9,462	10,86	10,76	10,4	9,94	9,11	10,0	9,19	8,39	9,72	9,14
TiO_2	4,31	5,719	5,043	6,84	4,70	4,22	4,55	2,69	3,64	4,46	4,12
MnO	0,226	0,244	0,265	0,308	0,313	0,293	0,276	0,214	0,271	0,241	0,249
Fe_2O_3	19,94	22,52	23,23	30,3	21,5	19,6	19,6	15,7	22,6	19,4	20,9
S	0,2177	0,2228	0,2192	0,2562	0,233	0,211	0,222	0,174	0,204	0,149	0,216
Cl	0,0237	0,0142	0,0377	0,0348	0,020	0,025	0,025	0,028	0,027	0,041	0,014
Sc	0,0035	0,0036	0,0044	0,0096	0,0053	0,0048	0,005	0,004	0,004	0,004	0,004
V	0,0532	0,046	0,0422	0,1247	0,0292	0,0244	0,0354	0,0298	0,0478	0,0344	0,0464
Cr	0,001	0,0005	0,0002	0,0041	<0.003	<0.003	<0.003	<0.003	0,0078	<0.003	<0.003
Ni	0,0046	0,0009	0,0014	0,0059	<0.002	<0.002	<0.002	0,0031	0,005	<0.002	<0.002
Cu	0,0096	0,0087	0,007	0,0773	0,0068	0,0048	0,0062	0,0054	0,0057	0,0042	0,0047
Zn	0,0141	0,0133	0,0159	0,0235	0,0181	0,0176	0,0159	0,0144	0,0181	0,0152	0,0179
Ga	0,0021	0,0019	0,0017	0,0023	0,0024	<0.002	<0.002	0,002	0,0028	0,0025	<0.002
Rb	0,0025	0,0006	0,0013	<0.001	0,0025	0,0034	0,0021	0,0046	0,0022	0,0055	0,0012
Sr	0,0414	0,042	0,0423	0,0204	0,044	0,0441	0,0434	0,0629	0,0453	0,0529	0,0574
Y	0,0028	0,0031	0,0034	0,0019	0,0038	0,0044	0,004	0,0025	0,0033	0,0023	0,0026
Zr	0,0052	0,0028	0,0028	0,0026	0,0091	0,0111	0,0097	0,0026	0,006	0,0039	0,0031
Nb	0,0011	0,0007	0,0006	0,0008	0,0015	0,0013	0,0013	<0.0007	<0.0007	0,001	<0.0007
Ba	0,0697	0,0476	0,0563	0,0206	0,1172	0,1446	0,1249	0,0792	0,0896	0,0675	0,0703
La	0,0021	0,0012	0,0021	<0.003	0,0042	0,0034	<0.003	<0.003	<0.003	<0.003	<0.003
Ce	0,0079	0,008	0,0081	0,0064	0,01	0,0079	0,0078	0,005	0,0074	0,0061	0,0062

Note: As, Mo, Sn, Pb, Sb, Bi, Th, U = below detection limit.

DH samples:
1 = R396 57.1-58.65
2 = R396 64.65-66.65
3 = R396 74.65-76.65
4 = R398 57.5
5 = R400 63.30-65.30
6 = R400 80.00-82.00
7 = R400 110.00-112.00
8 = R400 192.00-194.60
9 = R401 44.35-46.35
10 = R401 68.15-70.15
11 = R401 98.05-100.05

Barium feldspars have also been discovered in association with base metal mineralization (Coats et al. 1980, Chabu & Boulègue 1992) and barite deposits (Moro et al. 2001). Barium in feldspars, micas, and other silicates would be useful in mineral exploration; as such an occurrence may generally indicate the nearby presence of base metal sulphides and barite.

High Ba concentrations associated with potassium feldspar are also characteristic in the pyroxene-bearing granitoids (Lahti 1995) and base metal mineralization (Lahtinen & Johanson 1987) within Central Finland. However, very few Ba-rich silicate compositions have been reported associated with gabbroic intrusions (e.g., Bigi et al. 1993). This study focuses on the upper part of the Lumikangas intrusion, which according to Sarapää et al. (2005) is classified as subhedral medium-grained monzogabbro. The aim of this article is to present the mineralogical, textural and chemical characteristics of barium-bearing potassium feldspar and other related minerals and their possible genesis.

2 LUMIKANGAS GABBRO, KAUHAJOKI

The Kauhajoki gabbro province, which is situated in South Pohjanmaa, Finland, and is characterized as a host for Fe-Ti and apatite ore, has been a subject of various studies in recent years (e.g., Huuskonen & Kärkkäinen 1994, Kärkkäinen et al. 1997, Kärkkäinen & Appelqvist 1999, Sarapää et al. 2005). The Kauhajoki mafic to ultramafic intrusion complexes occur along the contact between the synorogenic (ca. 1890 Ma) Central Finland Granitoid Complex and the late- or post-orogenic (ca. 1870 Ma) granites (Figure 1) within the Proterozoic Svecofennian bedrock of western Finland (Kärkkäinen & Appelqvist 1999). The Lumikangas gabbro is one of several gabbroic bodies in the province of Kauhajoki that the Geological Survey of Finland (GTK) has explored as a potential source for titanium and phosphorous. The target was selected based on a regional geophysical anomaly on magnetic and gravity maps. According to further geophysical investigation, the gabbro body is 1.5 km long, 0.5 km wide, 300 to 500 m deep and covered with a 30 to 70 m thick overburden (Sarapää et al. 2005). During early bedrock mapping and ore exploration, the first drilling penetrated a layered gabbro containing 15 to 20 wt% of magnetite, apatite and ilmenite. In 2004, ground magnetic and gravity measurements were conducted based on which five drill holes (R396–401) along two profiles were drilled in the southern part of the intrusion. Based on the drilling results, the gabbro body dips 30o to the east, and is dissected into two blocks by reverse faulting.

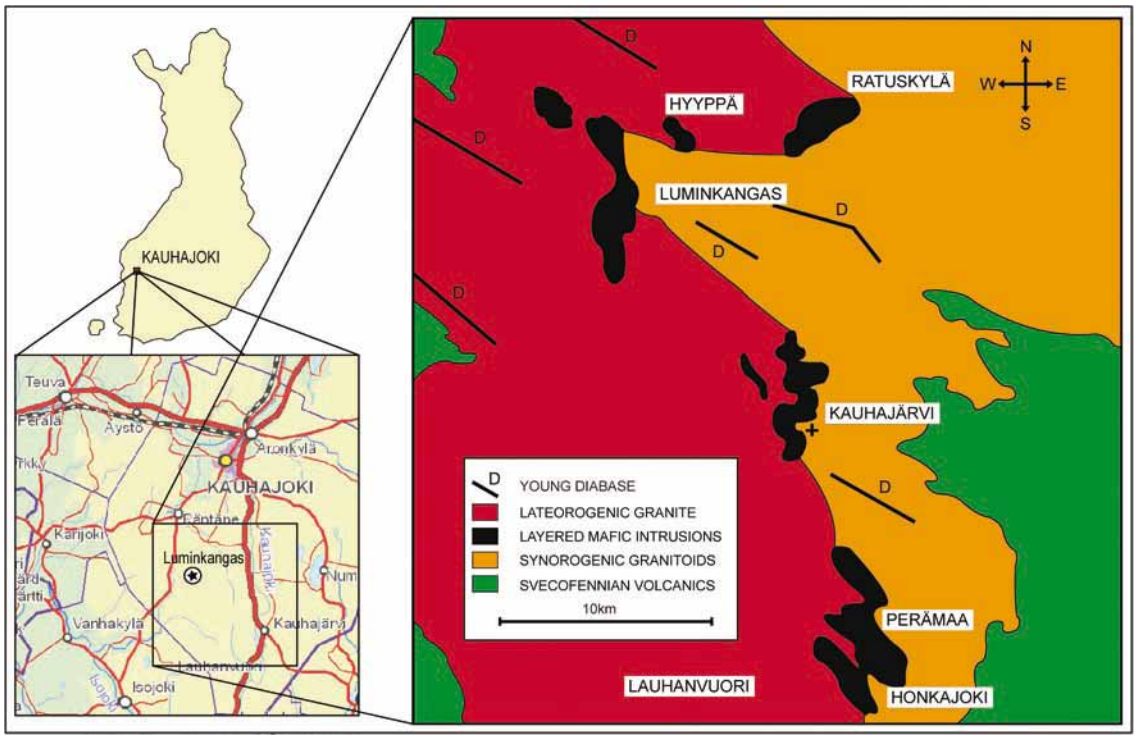

Figure 1. Location of Lumikangas at Kauhajoki and a generalized geological map (after Sarapää et al. 2005).

Data of extensive chemical analyses and susceptibility measurements were produced along the drill core samples. Polished thin-sections and mineral concentrates were prepared for petrographic analyses using a JEOL JSM5900LV scanning electron microscope (SEM) and a electron microprobe (EMP).

The mineral content and whole rock chemical analyses of the Lumikangas gabbro indicate a mafic to ultramafic complex with mainly gabbroic composition, where the primary mafic minerals (clinopyroxene, orthopyroxene and olivine) are partially metamorphosed and replaced by mainly altered mafic minerals (uralite), biotite group minerals, and minor chlorite. Generally, the rock has a subophitic or granular texture, which is still preserved. Lithologically, the Lumikangas gabbro is divided into two parts; the basal part of the intrusion is composed of dark medium-grained gabbro, gabbronorite, hornblende gabbro and olivine gabbro, and the upper part is composed of medium to coarse-grained monzogabbro and olivine monzogabbro (Sarapää et al. 2005).

3 MATERIALS AND METHODS

Mineralogical studies were conducted on drill core samples from DH398 at 57.5m and from DH400 at 63.9m, 81.0m, 111.9m, 138.7m, 141.6m, 149.2m, taken from the Lumikangas ilmenite-magnetite-apatite bearing gabbro in Kauhajoki, western Finland. Several high-quality polished thin-sections were prepared for examination using a reflected and transmitted light microscope, a scanning electron microscope (SEM) and an electron microprobe (EMP). These sections were examined for rock-forming minerals, mainly for alkali feldspar and plagioclase, and their textural relationships. Microphotographs of feldspar and related minerals were taken to illustrate observations on inclusions, exsolutions, alterations and other textural features. Ba-rich areas within feldspar grains can be identified by using back scattered electron (BSE) imaging due to the high atomic number of Ba. BSE images revealed microstructures of coexisting albite, potassium feldspar and Ba-rich potassium feldspar, and showed that the feldspar is often chemically heterogeneous.

The quantitative composition of coexisting feldspars, plagioclase and biotite group minerals was analysed using a Cameca Camebax SX50 Electron Microprobe (EMPA) equipped with four wavelength-dispersive spectrometers. Analyses were carried out at 15 kV and with a 20 nA probe current and a 10 µm spot size (beam diameter). Under these operating conditions the detection limit for Ba was 835 ppm. Analyses of feldspar also included MgO, Cr_2O_3, MnO, TiO_2, NiO, P_2O_5 and Cl. The values, however, are negligible and considered irrelevant in the calculation of end members. Electron microprobe analyses provide the composition of a given mineral only as weight percentages of the constituent oxides. The composition of potassium feldspar, Ba-rich potassium feldspar, hyalophane and Na-rich potassium feldspar are calculated based on a procedure given in Deer et al. (1992). Feldspar formulas are written with eight oxygens; hence, the numbers of anions are determined on the basis of eight oxygens, 8(O). After the number of ions in the formula was specified (Tables 2 and 3), the range of compositions between feldspar end-members (potassium feldspar = Orthoclase (Or), albite (Ab), anorthite (An) and celsian (Cn)) is obtained using major constituents (Ca, K, Na, Ba), for instance: Ab = Na/(Na+Ca+K+Ba).

4 RESULTS

4.1 Petrographic analysis

Generally, the rock-forming minerals are plagioclase, feldspar, biotite group minerals, altered mafic minerals (uralite), cummingtonite, Fe-Ti-oxides (ilmenite and magnetite), apatite, pyroxenes (cpx and opx), olivine and rarely titanite, calcite, sericite, chlorite and quartz. Clinopyroxene, orthopyroxene and olivine are partially altered to uralite and biotite group minerals. Oriented intergrowth between Fe-Ti-oxides, mainly ilmenite lamellae in magnetite, is common. Mafic minerals are closely associated with Fe-Ti-oxides, often in the form of micrographic (myrmecitic) intergrowth. Inclusions of apatite in Fe-Ti-oxides and silicates are a typical texture. Apatite chadacrysts occurring as fine subrounded and elongated structures and are enclosed by feldspar oikocrysts, which are typical for a poikilophitic texture. The silicate minerals comprise 75 to 95 vol% of the rock, whereas ilmenite, magnetite and apatite are minor constituents (Chernet et al. 2004). Prismatic to granular plagioclase grains are up to three mm in length and are commonly intermingled by sericite. Partially replaced plagioclase crystals exhibit deformed albite twinning and mottled extinction. Slight albitization of plagioclase is observed, mainly

indicated by indistinct albite twinning (Figure 2). Plagioclase also exhibits pericline twinning. Both pericline and albite twinning seem to combine in many plagioclase grains showing a checkerboard (tartan) twinning that gives a false appearance of microcline grid twinning (Figure 3). Some of the plagioclase crystals are zoned, although no clear replacement by alkali feldspar is evident (Figure 4).

Large irregular crystals of alkali feldspar are filling interstices between plagioclase crystals and other minerals (Figure 5). It is not uncommon to see alkali feldspar hosting pyroxene, biotite group minerals, altered mafic minerals (uralite), apatite, Fe-Ti-oxides, and even plagioclase. Most natural alkali feldspars are rather inhomogeneous, containing separate K-rich and Na-rich phases. Here, BSE images revealed textures of coexisting feldspars (potassium feldspar, barium-potassium feldspar, hyalophane, and albite/oligoclase). Barium-potassium feldspar is also distinguished as an antiperthitic structure with stringers and interlocking of hyalophane within Na-rich feldspar (Figure 6). Uniformly distributed microperthitic structures are also observed, which are oriented in thin plagioclase (albite-oligoclase) lamellae, isolated blebs and interlocks in barium-potassium feldspar (Figure 7). The distribution of Na-rich feldspar blebs in perthite and barium-potassium feldspar/hyalophane blebs in antiperthite is both regular and irregular and appears with different sizes and shapes. Grain boundaries of such inhomogeneous potassium

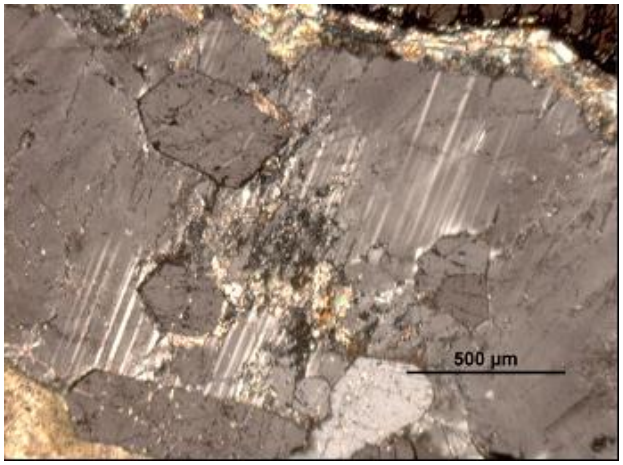

Figure 2. Non-contiguous polysynthetic twinning in albitic plagioclase. Crossed polarized light.

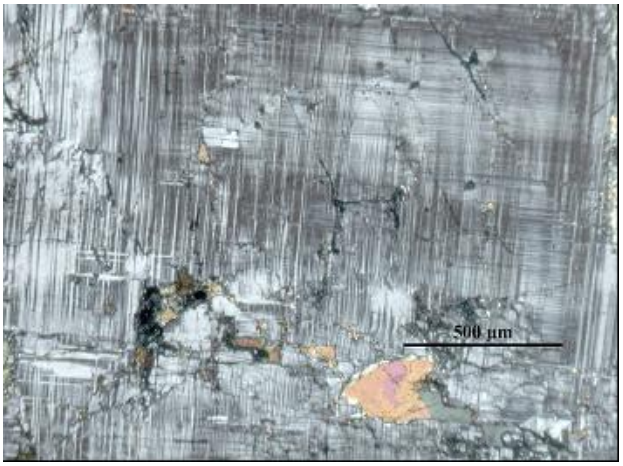

Figure 3. Checkerboard (tartan) twinning pattern in plagioclase. Crossed polarized light.

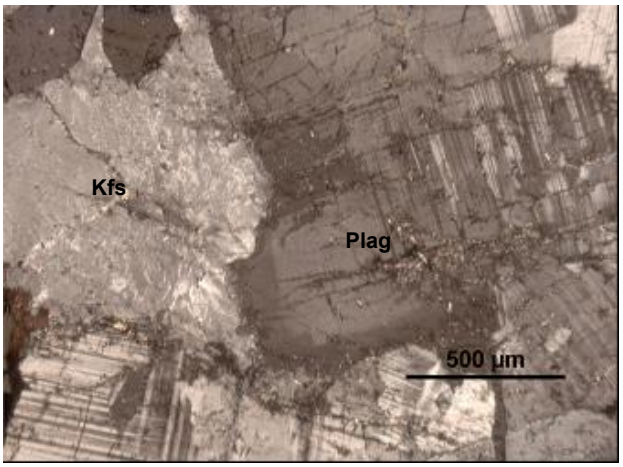

Figure 4. Optical zoning in plagioclase in the contact with potassium feldspar (Plag = plagioclase, Kfs = potassium feldspar). Crossed polarized light.

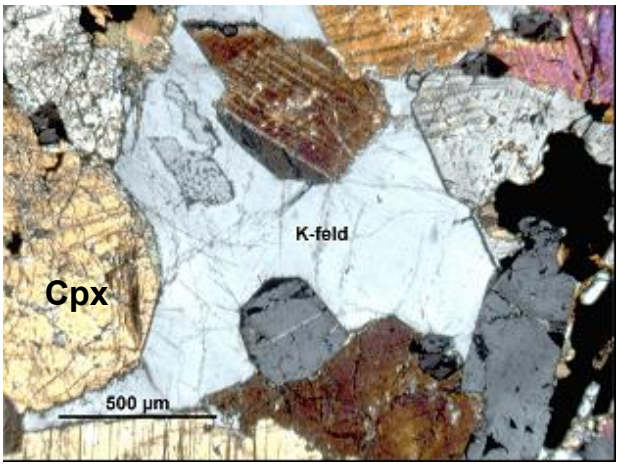

Figure 5. Large irregular crystal of potassium feldspar (Kfs) filling interstices between clinopyroxene (Cpx). Kfs contains 6 to 7.5 wt% BaO. Note: apatite (Apt). Crossed polarized light.

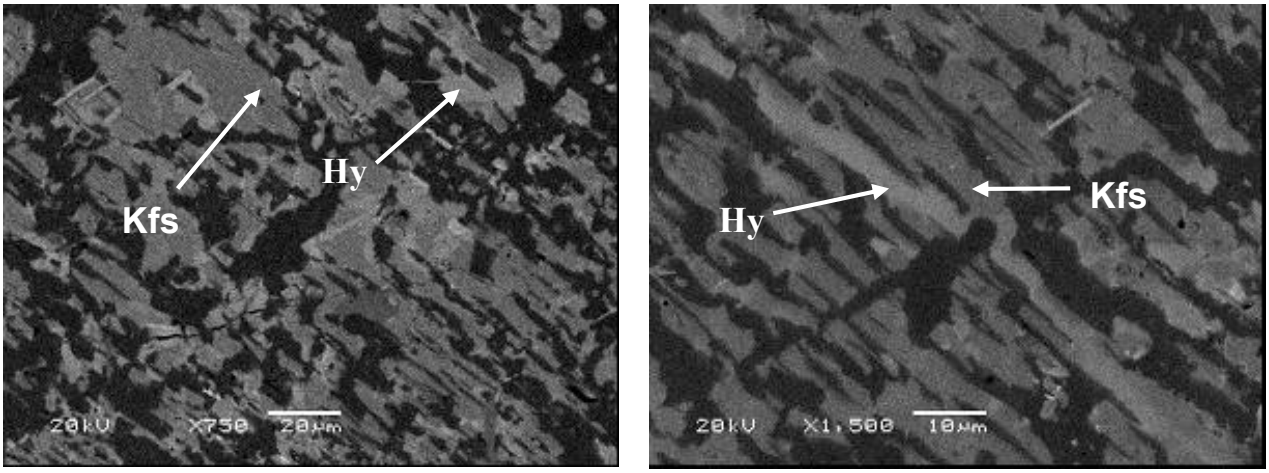

Figure 6. SEM-BSE images showing hyalophane (HY) intergrown with potassium feldspar (Kfs) containing less Ba in Na-rich feldspar (dark).

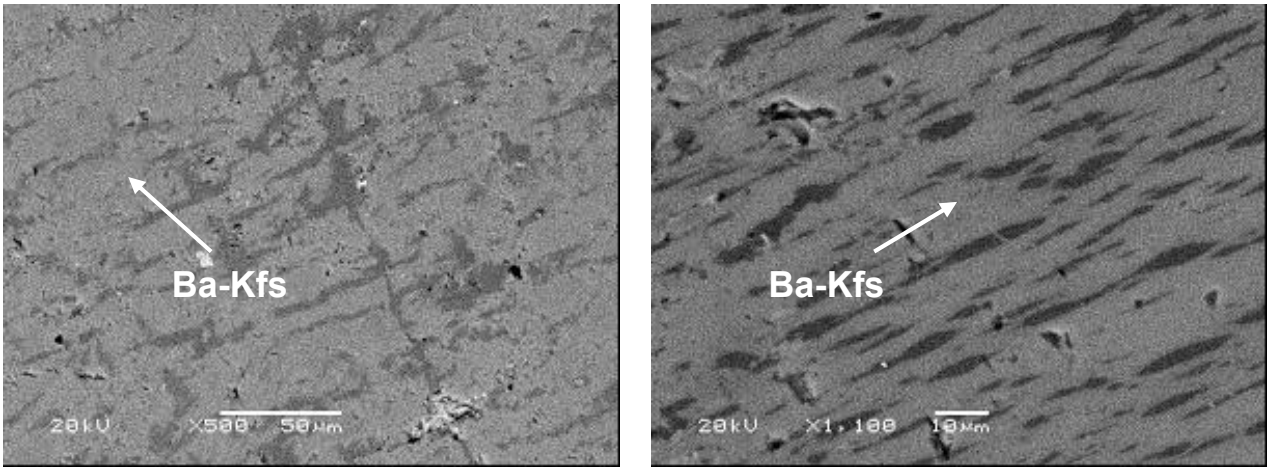

Figure 7. SEM-BSE images showing Ba-bearing potassium feldspar (Ba-Kfs) with perthitic Na-rich feldspar (dark). Ba-bearing potassium feldspar contains up to 6 wt% BaO.

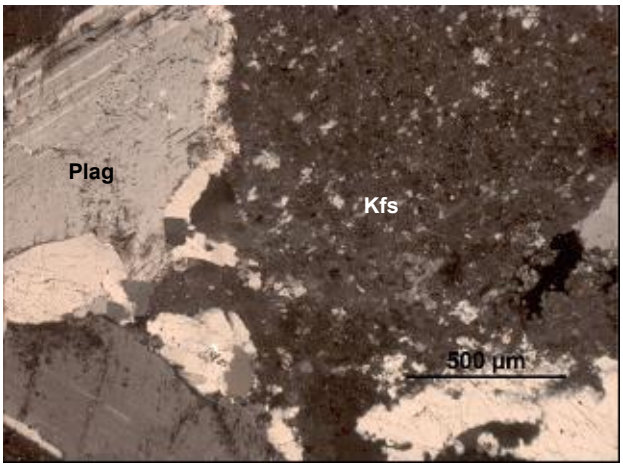

Figure 8. Grain contact between antiperthitic potassium feldspar and plagioclase surrounded by marginally grown quartz crystallites (Plag= Plagioclase, Kfs= Potassium feldspar). Crossed polarized light.

feldspar and plagioclase are often rimmed with quartz crystallites (Figure 8).

Alteration of mafic and ultramafic minerals, sometimes referred to as 'uralitization', is frequently observed. Biotite group minerals are also common silicate minerals, together with altered mafic minerals (uralite) often rimming ilmenite and magnetite. Olivine is observed in a few sections, commonly fractured, partially altered and associated with ilmenite and apatite. Veinlets of albite along with calcite and chlorite are locally observed crossing the rock-forming minerals.

4.2 Electron Microprobe Analysis (EMPA)

Potassium feldspar is often found to contain barium, giving barium-potassium feldspar and hyalophane compositions (Tables 2 and 3). Based on electron microprobe analyses, the K-rich feldspar seems to have an orthoclase composition and its BaO-content ranges from about 0.4 to 10.4 wt%. Although considerable variation in the BaO-content is encountered, the composition clearly includes the hyalophane composition described by De Pieri et al. (1977), Phillips & Griffen (1981), Deer et al. (1992) and Essene et al. (2005). Apparently, the Ba-concentration is correlated with the concentration of potassium. However, the increase or decrease in the K/Na ratio does not systematically correspond to an increase in the Ba-content. Instead, Ba-rich potassium feldspar seems to exhibit deficiency in silica (Table 2; Figure 9); a higher BaO-content corresponds to the lower SiO_2-content.

The barium-bearing potassium feldspar is chemically variable from one grain to another, and even within a single grain, due to its complex textural configuration. Potassium feldspar grains free of exsolved textures contain 2.1 to 7.6 wt% BaO. The composition corresponds to both barium-potassium feldspar ($Cn_{4–12}An_{0–3}Ab_{14–28}Or_{63–75}$) and hyalophane (e.g., $Cn_{15}Ab_{16}Or_{69}$). In the antiperthite structure, where the host is Na-rich feldspar ($An_{6–9}Ab_{91–94}Or_{0–1}$), the BaO-content of the potassium feldspar often ranges between 6 to 10.4 wt%, referring to antiperthititic barium-potassium feldspar (e.g., $Cn_{13}Ab_{18}Or_{69}$) and antiperthitic hyalophane ($Cn_{18–21}An_{0–1}Ab_{10–19}Or_{62–71}$). In the perthite exsolution intergrowth, the BaO-content of the potassium feldspar ranges from 0.5 to 5.6 wt%, referring to perthitic barian potassium feldspar. The composition of the exsolved lamellae in the perthite structure is oligoclase ($Cn_{0–1}An_{16–29}Ab_{71–83}Or_{0–3}$). The BaO-content is lowest in the mesoperthite structure, where potassium feldspar ($Cn_1An_0Ab_{3–7}Or_{92–96}$) and albite ($An_6Ab_{93}Or_1$) intergrowth are in approximately equal proportions. BSE images from SEM indicate islands of Ba-content in the alkali feldspar of up to 16 wt% BaO (Figure 10).

In many cases, the albite and Carlsbad-twinning in the plagioclase crystals begin to fade (Figure 2). In

Table 2. Electron microprobe analysis (by Lassi Pakkanen) of Ba-bearing feldspars (as wt%), atoms based on 8 oxygens/unit cell and calculated end members.

	1	2	3	4	5	6	7	8	9	10	11	12
SiO_2	58,92	60,20	63,27	58,33	55,22	56,57	58,53	58,87	66,26	66,75	67,05	65,21
Al_2O_3	20,27	19,72	19,65	19,93	20,59	20,31	19,56	19,85	20,92	20,77	20,48	21,86
FeO	0,06	0,03	0,02	0,06	0,01	0,01	0,02	0,08	0,01	0,10	0,04	0,09
CaO	0,52	0,04	0,56	0,001	0,02	0,05	0,12	0,09	1,83	1,37	1,30	2,67
Na_2O	2,37	1,48	3,09	1,71	1,01	1,01	1,89	1,82	10,76	11,07	11,13	9,82
K_2O	10,12	11,89	10,95	10,86	10,58	11,16	9,23	10,91	0,15	0,14	0,05	0,22
SrO	0,07	0,05	0,02	BDL	0,18	0,08	0,01	BDL	0,07	0,06	0,17	0,30
BaO	6,40	5,84	2,14	7,64	10,42	9,54	8,76	6,71	0,02	0,08	0,02	0,09
Total	98,73	99,24	99,69	98,54	98,04	98,73	98,12	98,33	100,02	100,35	100,24	100,26
Si	2,84	2,89	2,94	2,86	2,78	2,81	2,88	2,86	2,91	2,92	2,94	2,87
Al	1,15	1,12	1,07	1,15	1,22	1,19	1,13	1,14	1,08	1,07	1,06	1,13
Fe	0,003	0,001	0,001	0,003	0,0002	0,0005	0,0008	0,003	0,0005	0,004	0,001	0,003
Ca	0,03	0,002	0,03	BDL	0,001	0,003	0,01	0,004	0,09	0,06	0,06	0,13
Na	0,22	0,14	0,28	0,16	0,10	0,10	0,18	0,17	0,92	0,94	0,94	0,84
K	0,62	0,73	0,65	0,68	0,68	0,71	0,58	0,68	0,01	0,01	0,003	0,01
Sr	0,002	0,001	0,0004	BDL	0,01	0,002	0,0002	BDL	0,002	0,002	0,004	0,01
Ba	0,12	0,11	0,04	0,15	0,21	0,19	0,17	0,13	BDL	0,001	0,0004	0,002
Total	4,99	4,99	5,00	4,99	5,00	5,00	4,94	4,98	5,01	5,01	5,01	4,98
Cn	12,19	11,24	3,93	14,84	20,88	18,70	18,07	13,04	0,04	0,14	0,04	0,17
An	2,71	0,21	2,80	0,01	0,13	0,26	0,68	0,45	8,50	6,32	6,06	12,85
Ab	22,31	14,07	27,98	16,46	10,03	9,83	19,27	17,48	90,61	92,76	93,62	85,73
Or	62,79	74,48	65,29	68,68	68,96	71,20	61,98	69,02	0,85	0,78	0,27	1,25

Note: Ba-K-feldspar (1,2,3), hyalophane (4), antiperthite hyalophane (5,6,7), antiperthite Ba-K-feldspar (8), antiperthite albite (9,10,11), antiperthite oligoclase (12), Cn = Celsian, An = anorthite, Ab = albite, Or = orthoclase, BDL = below detection limit.

Table 3. Electron microprobe analysis (by Lassi Pakkanen) of Ba-bearing feldspars (as wt%), atoms based on 8 oxygens/unit cell and calculated end members.

	13	14	15	16	17	18	19	20	21	22	23	24
SiO_2	61,67	64,26	61,13	59,55	62,95	64,20	62,18	60,60	64,46	64,69	66,99	67,30
Al_2O_3	19,13	18,85	19,26	19,76	23,07	22,52	23,04	24,75	18,25	18,32	20,51	20,16
FeO	BDL	0,04	0,02	0,04	0,01	0,14	0,13	0,08	BDL	BDL	BDL	BDL
CaO	0,02	0,003	0,06	0,15	4,15	3,51	4,14	5,97	0,003	0,03	1,19	1,20
Na_2O	1,47	1,32	1,59	1,68	9,16	9,75	8,81	8,25	0,31	0,73	10,98	11,13
K_2O	13,07	14,09	12,28	11,44	0,23	0,11	0,55	0,06	15,58	14,92	0,19	0,16
SrO	BDL	BDL	BDL	BDL	0,03	0,14	0,19	0,17	BDL	BDL	BDL	0,08
BaO	3,45	0,52	4,49	5,57	0,12	0,16	0,51	0,06	0,59	0,36	BDL	BDL
Total	98,81	99,09	98,85	98,19	99,72	100,53	99,55	99,94	99,19	99,05	99,85	100,03
Si	2,93	2,98	2,92	2,88	2,79	2,82	2,78	2,70	3,00	3,00	2,94	2,95
Al	1,07	1,03	1,08	1,13	1,21	1,17	1,21	1,30	1,00	1,00	1,06	1,04
Fe	BDL	0,002	0,001	0,001	0,0003	0,01	0,005	0,003	BDL	BDL	BDL	BDL
Ca	0,0009	0,0001	0,0031	0,01	0,20	0,17	0,20	0,28	0,0001	0,0017	0,06	0,06
Na	0,14	0,12	0,15	0,16	0,79	0,83	0,76	0,71	0,03	0,07	0,94	0,95
K	0,79	0,83	0,75	0,71	0,01	0,01	0,03	0,003	0,93	0,88	0,01	0,01
Sr	BDL	BDL	BDL	BDL	0,001	0,004	0,01	0,004	BDL	BDL	BDL	BDL
Ba	0,06	0,01	0,08	0,11	0,002	0,003	0,01	0,001	0,01	0,01	BDL	BDL
Total	5,00	4,98	4,98	4,99	5,00	5,00	5,00	5,01	4,97	4,96	5,01	5,00
Cn	6,46	0,98	8,55	10,81	0,21	0,27	0,90	0,11	1,12	0,68	0,00	0,00
An	0,09	0,01	0,31	0,79	19,70	16,45	19,78	28,44	0,01	0,17	5,59	5,58
Ab	13,68	12,37	15,01	16,15	78,79	82,66	76,21	71,10	2,92	6,90	93,36	93,56
Or	79,77	86,63	76,12	72,25	1,30	0,62	3,11	0,35	95,95	92,24	1,05	0,86

Note: Perthite Ba-K-feldspar (13,14,15,16), perthite oligoclase (17,18,19,20), mesoperthite K-felsdpar (21,22), mesoperthite albite (23,24), Cn = celsian, An = anorthite, Ab = albite, Or = orthoclase, BDL = below detection limit.

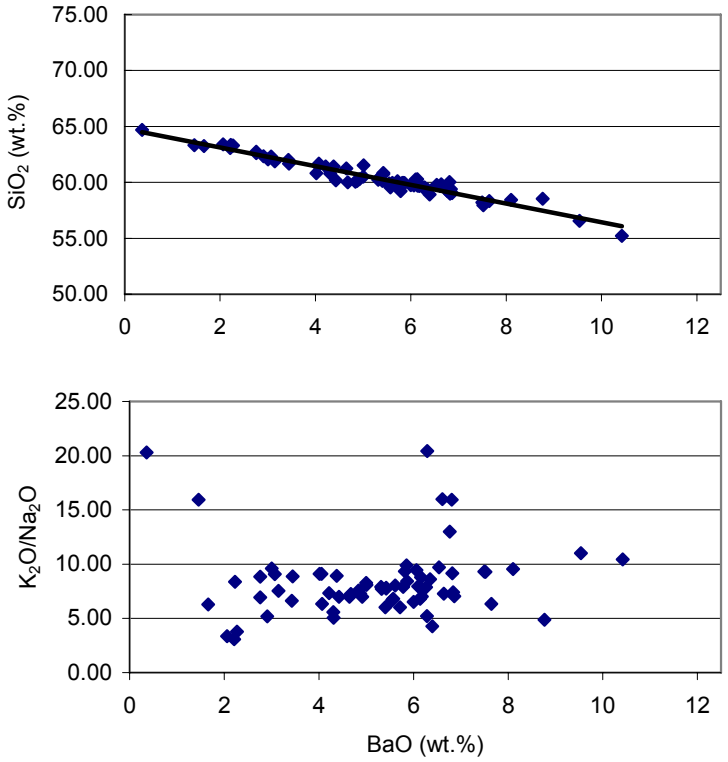

Figure 9. Graph showing the correlation of SiO_2 (above) and the K_2O/Na_2O ratio (below) versus the BaO content in potassium feldspar, as measured by EPMA.

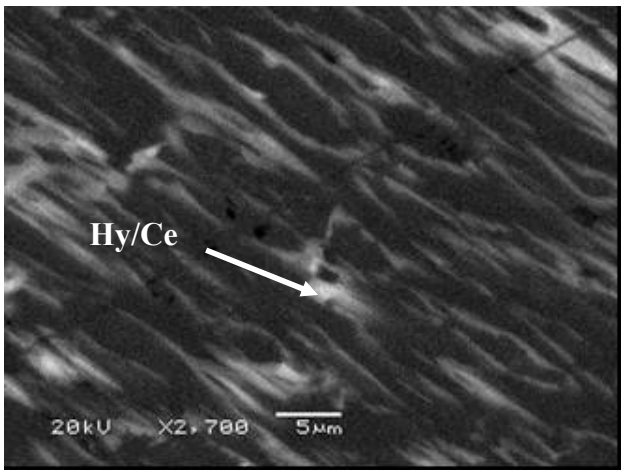

Figure 10. SEM-BSE image od hyalophane/celsian (Hy/Ce) with up to 16 wt% BaO (SEM) in antiperthitic potassium feldspar.

this figure, the plagioclase crystals exhibit a lack of zonation and become more sodic in composition at the expense of Al and Ca (Table 4). The composition of plagioclase corresponds more to andesine.

Results of analysis of biotite group minerals indicate a content of BaO ranging from 0.1 to 1.27 wt% (Table 5). The clinopyroxene has a ferro-augite composition, which is typical for gabbroic rock, characterized by low Al_2O_3 (about 1.8 wt%) and TiO_2-contents (commonly <0.5 wt%). A few grains display higher Al_2O_3-contents of up to 2.2 wt% and higher TiO_2-contents of up to 0.8 wt%.

Table 4. Electron microprobe analysis (by Lassi Pakkanen) of plagioclase (as wt%).

	1	2	3	4	5	6	7	8
SiO_2	55,11	55,26	56,26	56,44	59,99	57,36	55,71	55,32
TiO_2	0,05	0,07	0,05	0,07	0,02	0,06	0,04	0,07
Al_2O_3	28,12	28,18	27,66	27,37	25,01	26,74	27,78	28,02
Cr_2O_3	0,0001	0,000	0,03	0,03	BDL	0,03	0,01	0,02
P_2O_5	0,04	0,04	0,005	0,02	0,003	0,02	0,05	0,01
FeO	0,14	0,16	0,10	0,04	0,02	0,12	0,09	0,11
MnO	0,01	0,02	0,03	BDL	0,001	0,05	0,01	0,01
MgO	0,01	0,01	0,01	0,005	0,01	0,01	0,01	0,01
CaO	9,96	10,06	9,34	9,17	6,49	8,51	9,74	10,01
Na_2O	5,65	5,58	6,12	6,21	7,79	6,59	5,98	5,61
K_2O	0,15	0,19	0,05	0,08	0,10	0,18	0,13	0,15
SrO	0,15	0,13	0,18	0,20	0,23	0,07	0,10	0,09
BaO	0,08	0,10	0,12	0,08	0,06	0,19	0,10	0,10
NiO	0,02	0,01	0,01	0,02	0,05	0,01	0,02	0,003
Cl	0,02	0,03	0,02	0,03	0,03	0,03	0,02	0,02
Total	99,50	99,82	99,99	99,77	99,81	99,98	99,79	99,54

Note: Plagioclase (1-8), BDL = below detection limit.

Table 5. Electron microprobe analysis (by Lassi Pakkanen) of biotite (as wt%).

	1	2	3	4	5	6	7	8
SiO_2	36,12	33,34	33,13	33,78	34,74	35,04	33,79	33,95
TiO_2	3,03	4,23	3,68	3,93	4,69	4,87	3,14	4,63
Al_2O_3	13,99	14,31	14,54	14,22	13,77	13,69	14,15	13,66
Cr_2O_3	0,01	BDL	BDL	BDL	BDL	0,04	BDL	BDL
P_2O_5	0,04	0,01	0,01	0,03	BDL	0,03	0,02	0,03
FeO	20,11	28,46	28,90	28,66	26,01	25,50	28,71	26,99
MnO	0,10	0,09	0,13	0,13	0,05	0,07	0,11	0,07
MgO	11,20	4,36	4,20	4,40	6,07	6,46	5,08	5,69
CaO	0,05	0,03	0,05	0,02	0,01	0,18	0,10	0,03
Na_2O	0,12	0,09	0,09	0,09	BDL	0,02	0,002	0,004
K_2O	8,86	8,08	8,39	8,53	8,99	8,88	8,53	8,38
SrO	BDL	BDL	0,02	BDL	0,002	BDL	0,01	BDL
BaO	0,58	1,27	1,00	0,69	0,08	0,18	0,64	1,17
NiO	0,03	0,01	0,02	0,01	0,01	0,00	0,01	0,01
F	BDL	BDL	BDL	BDL	BDL	BDL	BDL	BDL
Cl	0,09	0,10	0,13	0,13	0,17	0,15	0,17	0,18
Total	94,32	94,39	94,29	94,61	94,60	95,11	94,45	94,80

Note: Biotite (1-8), BDL = below detection limit.

5 DISCUSSION

Feldspars are generally considered as barium varieties when their barium content exceeds approximately 2 wt% BaO (Deer et al. 1992). The composition range for hyalophane, however, has recently been defined by Essene et al. (2005) to be within 15 to 75 % of the celsian molecule ($BaAl_2Si_2O_8$). Barium feldspars usually occur in association with manganese deposits (Deer et al. 1992, Brobst 1994), but have also been observed to occur in different geological environments. Mäkipää (1976) noted Sr and Ba rich feldspar from the Korsnäs Pb-REE deposit containing up to 6.15 wt% SrO and up to 7.73 wt% BaO. Barium-bearing feldspar has also been described by Lahtinen & Johanson (1987) from the Pukkiharju base-metal mineralization with a typical hyalophane composition ($Cn_{22–25}Ab_{22–24}Or_{52–55}$). Based on alteration and texture, the hyalophane grains were interpreted to have metamorphic origin.

The Lumikangas gabbro, which is the host of disseminated Fe-Ti-oxides and apatite mineralization, is partially metamorphosed to amphibolite facies, replaced mainly by altered mafic minerals (uralite) and biotite group minerals, and has also been affected by slight albitization and sericitization of plagioclase. Textural imprints suggest early crystallization of apatite, partially reserved mafic minerals (opx, cpx, and olivine) and Fe-Ti oxides. The simultaneous crystallization of these minerals could also be explained by close correlation of Ti, P and Mg (Sarapää et al. 2005) and a random micrographic intergrowth of Fe-Ti-oxides with mafic minerals. Kärkkäinen & Appelqvist (1999) also discussed the coeval crystallization of apatite, Fe-Ti-oxides and Fe-Mg-silicates as being characteristic in the Kauhajärvi gabbro, which is one of several mafic to ultramafic intrusion complexes within the Kauhajoki gabbro province. The oriented intergrowth exhibited by Fe-Ti ore minerals (magnetite and ilmenite) arising from unmixing of a solid solution, is a direct consequence of crystallization. Uralite and biotite group minerals, chlorite and sericite might indicate a regional metamorphism, which eventually has been initiated either by the introduction of hydrothermal fluids or by late-stage fluids left over from the final crystallization of the magmatic rock. The occurrence of the regional reverse faulting structure, the presence of gabbro-pegmatoid and metadiabase dikes (Sarapää et al. 2005) as well as the macro- and microscale fracturing might have opened up the system to the movement of fluids.

In a normative quartz-orthoclase-plagioclase triangular diagram after Streckeisen (1976), most Lumikangas samples fall within the monzogabbro field containing more than 10 vol% alkali feldspar component (Sarapää et al. 2005). These alkali feldspar crystals seem to be magmatic in origin due to: (1) the presence of orthoclase (Figure 5), which is often the original potassium feldspar in magmatic rocks (Collins 1997); (2) the straight sharp contacts of potassium feldspar with other crystals (Figure 5), and (3) the presence of a solid solution of Na, Ca, and K in high-temperature alkali feldspars (orthoclase and anorthoclase) and the subsequent exsolution of Na and Ca to form perthite. In the perthite the plagioclase lamellae are evenly distributed throughout the potassium feldspar with diverse patterns (Figure 7) (Collins 1997). Similar relationships apply to antiperthite, in which Na-rich feldspar is the host and potassium feldspar is the exsolved component (Figure 6). Furthermore, the fact that most of the alkali feldspar grains are interstitial and are found to host most of the silicate minerals indicates the source to be late-stage magmatic crystallization. Quartz grains are often found along the border of the microperthite. These quartz grains are interstitial and look like last-stage crystallization from the melt together with the alkali feldspar. This might also indicate that the rock locally is a primary monzogabbro.

The structural composition of the alkali feldspar is often intergrown phases of orthoclase and albite/oligoclase. The orthoclase variety is rich in barium (0.36 to 10.4 wt% BaO) that further includes the hyalophane composition ($Cn_{1–21}An_{0–3}Ab_{3–28}Or_{62–96}$). The coexisting or unmixing behaviour of two to four such phases has been described by many authors, including e.g., Nakano (1979), Viswanathan & Kielhorb (1983), Viswanathan & Harneit (1989), Chabu & Boulègue (1992) and Essene et al. (2005). The compositional data of hyalophane (Tables 2 and 3) also indicate a substantial content of albite. In the presence of albite, hyalophane in low-grade rocks has only 5 to 10 % Ab-molecules, whereas it may contain 25 to 35 % Ab-molecules in high-grade rocks (Bühn et al. 1995, Essene et al. 2005). Hyalophane in the Lumikangas gabbro contains 10 to 22 % Ab-molecules. This content might indicate hyalophane in medium-grade rocks where the mafic to ultramafic rocks were partially transformed to amphibolites due to metamorphism caused by late-stage magmatic fluid. The high content of Ba in the potassium feldspar indicates a high concentration of Ba in the late-stage magma fluid. The absence of sulphate in the fluids probably caused the formation of barium feldspars instead of barite. Biotite group minerals are rich in Ba (up to 1.27 wt% BaO) and Ti (3 to 4.8 wt% TiO_2). The Ba^{2+}-ion has the same size as the K^+-ion and therefore, will substitute for K in both, potassium feldspar and biotite group minerals. In contrast, the Ba^{2+}-ion is too large to substitute

for Na- or Ca-ions, which explains the lack of Ba in plagioclase or albite.

Albitization is a common reaction in all rock settings (Perez & Boles 2005) and reflects mass transfer (Boles 1982, Aagaard et al. 1990, Morad et al. 1990), which causes chemical changes. The gradual withering of albite twinning (Figure 2) and the change of some labradorite composition to andesine (Table 4) indicate that slight albitization has taken place in plagioclase. However, complete transformation of plagioclase to albite was not observed. Late-stage magmatism from the melt as well as late hydrothermal fluid introduction might also allow albitization of the plagioclase. Although the presence of plagioclase with normal zonation is a logical indication of magmatic origin (Karsli et al. 2004, L'heureux & Fowler 1994), here zoning is observed in plagioclase in contact with alkali feldspar (Figure 4). In this case, zoning might be secondary and caused by the plagioclase interaction with late-stage fluid. The common occurrence of an antiperthitic structure over a perthitic one and the formation of late-stage albite veinlets might support the presence of more Na than K in the late magmatic melt. While consuming Na, Si and H, albitization releases Ca and Al (Perez & Boles 2005). The rarely occurring calcite, chlorite and secondary mica might be precipitated from the released Ca and Al and are the consequences of the albitization of plagioclase (Wilson et al. 2000).

No clear evidence has been documented for the rock-forming minerals to have been subjected to local metasomatism for the formation of alkali feldspar. Replacement of plagioclase by alkali feldspar was not clearly observed. The plagioclase inclusions in alkali feldspar and in antiperthetic structures have no optical continuity with adjacent plagioclase crystals. Although a few dispersed quartz vermicules were observed in alkali feldspar, the formation of ghost myrmecite was not clear. Due to such facts, local potassium metasomatism was ruled out.

6 CONCLUSIONS

The following conclusions can be drawn from this study:

1) Compositionally unusual Ba-rich alkali feldspars (0.36 to 10.4 wt% BaO) of complex texture have been found in the Lumikangas ilmenite-magnetite-apatite mineralized gabbro. The coexisting phases in alkali feldspar are potassium feldspar/barian orthoclase, hyalophane, albite and oligoclase, which show a range of compositions.

2) Based on studies of compositions and textures, alkali feldspar is believed to be the latest crystallized phase from the magmatic melt, which also contains a high concentration of barium.

3) The secondary zoning along the contact with alkali feldspar, the gradual withering of albite twinning and the transformation of plagioclase to a more sodic component might be a result of late-stage magmatic activity. The abundance of antiperthitic over perthitic structures might support the presence of more Na than K in the late magmatic melt.

4) Simultaneous crystallization of apatite, Fe-Ti-oxides and Fe-Mg-silicates is characteristic of the Lumikangas gabbro.

5) Altered mafic minerals (uralite), biotite group minerals and chlorite are commonly formed as an alteration product of primary Fe-Mg-silicates during the late-stages of the magmatic crystallization, when water becomes enriched in the residual magma.

7 ACKNOWLEDGMENTS

I would like to thank Dr. Olli Sarapää, who provided the drill core samples and Lassi Pakkanen for his assistance with the EMP analysis. I am grateful to Maarten Broekmans, Norwegian Geological Survey (NGU) and Seppo Lahti, Geological Survey of Finland (GTK) for their valuable suggestions, from which this paper is greatly benefited. Special thanks to Stefanie Lode for editing the manuscript. Personal thanks to my colleagues (Marja Lehtonen, Bo Johanson, Jukka Marmo, Hugh O'Brien) at GTK for all-round support.

REFERENCES

Aagaard, P., Egeberg, P. K., Saigal, G. C., Morad, S. & Bjørlykke, K. 1990. Diagenetic albitization of detrital K-feldspars in Jurassic, Lower Cretaceous and Tertiary Clastic reservoir rocks from offshore Norway, II. Formation water chemistry and kinetic considerations. Journal of Sedimentary Petrology 60, 575–581.

Bigi, S., Brigatti, M. F., Mazzucchelli, M. & Rivalenti, G. 1993. Crystal chemical variations in Ba-rich biotites from gabbroic rocks of lower crust (Ivrea Zone, NW Italy). Contribution to mineralogy and petrology 113, 87–99.

Bjoerlykke, K. O. & Griffin, W. L. 1973. Barium feldspars in Ordovician sediments, Oslo region, Norway. Journal of Sedimentary Research 43(2), 461–465.

Boles, J. R. 1982. Active albitization of plagioclase, Gulf Coast Tertiary. American Journal of Science 282, 165–180.

Brobst, D. A. 1994. Barium Minerals. In: Carr, D. D. (ed.) Industrial Minerals and Rocks, 6th edition, Society for Mining. Metallurgy and Exploration, 125–134.

Bühn, B., Okrusch, M., Woermann, E., Lehnert, K. & Hoernes. S. 1995. Metamorphic evolution of Neo-protrozoic manganese formations and their country rocks at Otjosondu, Namibia. Journal of Petrology 36, 463–496.

Chabu, M. & Boulègue, J. 1992. Barian feldspar and muscovite from the Kipushi Zn-Pb-Cu deposit, Shaba, Zaire. Canadian Mineralogist 30, 1143–1152.

Chernet, T., Sarapää, O., Johanson, B. & Pakkanen, L. 2004. Petrological and mineralogical studies on Lumikangas ilmenite-magnetite-apatite bearing gabbro, Kauhajoki, Western Finland. Geological Survey of Finland, unpublished report M19/1234/2004/1/42. 24 p.

Coates, J. S., Smith, C. G., Fortey, N. J., Gallagher, M. J., May, F. & McCourt, W. J. 1980. Strata-bound barian-zinc mineralization in Dalradian schist near Aberfeldy, Scotland. Inst. Min. Metall., Trans. B89, 110–122.

Collins, L. G. 1997. Contrasting characteristics of magmatic and metasomatic granites and the myth that granite plutons can be only magmatic. Myrmekite, retrieved from www.csun.edu/~vcgeo005/mobility.htm

Deer, W. A., Howie, R. A. & Zussman, J. 1992. An introduction to the rock forming minerals. 2nd ed. Burnt Mill: Longman. 696 p.

De Pieri, R., Quareni, S. & Hall, K. M. 1977. Refinement of the structures of low and high hyalophanes. Acta Crystallographica 33, 3073–3076.

Essene, E. J., Claflin, C. L., Giorgetti, G., Mata, P. M., Peacor, D. R., Árkai, P. & Rathmell, M. A. 2005. Two-, three- and four-feldspar assemblages with hyalophane and celsian: implications for phase equilibria in BaAl2Si2O8–CaAl2Si2O8–NaAlSi3O8–KAlSi3O8. European Journal of Mineralogy 17(4), 515–535.

Frondel, C., Ito, J. & Hendricks, J. G. 1966. Barium feldspars from Franklin, New Jersey. American Mineralogist 51, 1388–1393.

Huuskonen, M. & Kärkkäinen, N. 1994. An exploration of Ti-P gabbros around the Lahavuori granite: mapping of high altitude aeromagnetic anomalies and the Hyyppä intrusion (original title in Finnish). Geological Survey of Finland, unpublished report M 19/1234/94/1/10. 13 p.

Kärkkäinen, N., Sarapää, O., Huuskonen, M., Koistinen, E. & Lehtimäki, J. 1997. Ilmenite exploration in western Finland and the mineral resources of the Kälviä deposit. In: Autio, S. (ed.) Geological Survey of Finland, Special paper 23, 15–24.

Kärkkäinen, N. & Appelqvist, H. 1999. Genesis of a low-grade apatite-ilmenite-magnetite deposit in the Kauhajärvi gabbro, western Finland. Mineralium Deposita 34, 754–769.

Karsli, O., Aydin, F. & Sadiklar, M. B. 2004. Magma Interaction Recorded in Plagioclase Zoning in Granitoid Systems, Zigana Granitoid, Eastern Pontides, Turkey. Turkish Journal of Earth Sciences 13, 287–305.

Lahti, S. I. 1995. Mineralogy and geochemistry of the vaaraslahti pyroxene granitoid in Pielavesi, Finland. Bulletin of Geological Survey of Finland 382, 5–25.

Lahtinen, R. & Johanson, B. 1987. Barium feldspar from Pukkiharju base-metal mineralization, central Finland. Bulletin of the Geological Society of Finland 59, 77–80.

L'Heureux, I. & Fowler, A. D. 1994. A nonlinear dynamical model of oscillatory zoning in plagioclase. American Mineralogist 79, 885–891.

Mäkipää, H. 1976. Korsnäsin strontium-maasälvästä. M.Sc. thesis, Helsinki University. 183 p.

Morad, S., Morten, B., Knarud, R. & Nystuen, J. 1990. Albitization of detrital plagioclase in Triassic reservoir sandstones from the Snorre Field, Norwegian North Sea. Journal of Sedimentary Petrology 60, 411–425.

Moro, M. C., Cembranos, M. L. & Fernandez, A. 2001. Celsian, (Ba,K)-feldspar and cymrite from Sedex barite deposits of Zamora, Spain. Canadian Mineralogist 39(4), 1039–1051.

Nakano, S. 1979. Intergrowth of barium microcline, hyalophane and albite in the barium-containing alkali feldspar from Nada-Tamagawa Mine, Iwate Prefecture, Japan. Mineral. Journal 9, 409–416.

Němec, D. 1975. Barium in K-feldspar megacrysts from granitic and syenitic rocks of the Bohemian Massif. TMPM Tschermaks Min. Petr. Mitt. 22, 109–116.

Perez, R. J. & Boles, J. R. 2005. An empirically derived kinetic model for albitization of detrital plagioclase. American Journal of Science 305, 312–343.

Phillips, W. R. & Griffen, D. T. 1981. Optical Mineralogy, The nonopaque minerals. San Francisco: Freeman and Company. 677 p.

Sarapää, O., Kärkkäinen, N., Chernet, T., Lohva, J. & Ahtola, T. 2005. Exploration results and mineralogical studies on the Lumikangas apatite-ilmenite gabbro, Kauhajoki, Western Finland. In: Autio, S. (ed.) Geological Survey of Finland, Special paper 38, 31–41.

Shmakin, B. M. 1979. Composition and structural state of K-feldspars from some U.S. pegmatites. American Mineralogist 64, 49–56.

Streckeisen, A. 1976. To each plutonic rock its proper name. Earth Science Reviews, v. 12, 1–33.

Viswanathan, K. & Kielhorn, H. M. 1983. Variation in the chemical composition and lattice dimensions of (Ba,K,Na)-feldspar from Othososndu, Namibia and their significance. American Mineralogist 68, 112–121.

Viswanathan, K. & Harneit, O. 1989. Solid-solution and unmixing in the feldspar system, albite (NaAlSi3O8)-celsian (BaAl2Si2O8). European Journal of Mineralogy, 1, 239–248.

Wilson, A., Boles, J. & Garven, G. 2000. Calcium mass transport and sandstone diagenesis during compaction-driven flow: Stevens Sandstone, San Joaquin Basin, California. Geological Society of America, Bulletin 112, 845–856.

www.gtk.fi
info@gtk.fi

As very few Ba-rich silicate compositions have been reported associated with gabbroic intrusions, the unusual concentration of potassium and barium in the Lumikangas ilmenite-magnetite-apatite mineralized gabbro is described. The presence of magmatic alkali feldspar and the coexistence of potassium feldspar and hyalophane are of considerable petrographic interest in unravelling clues to the crystallization of the mineralized gabbro. Moreover, this study and interpretation might have significant implications for the development of exploration strategies for minerals other than Fe-Ti bearing ones in these types of terrenes and related rocks.

ISBN 978-952-217-117-7 (PDF)
ISSN 0781-4240